Agreement INGV-DPC 2007-2009

Project S1: Analysis of the seismic potential in Italy for the evaluation of the seismic hazard

Responsibles: Salvatore Barba, Istituto Nazionale di Geofisica e Vulcanologia, and Carlo Doglioni, Università di Roma "La Sapienza"

http://groups.google.com/group/INGV-DPC-2007-S1
(restricted access)

Deliverable # 3.01.2
Slip rate data of seismogenic sources included in DISS

May 31st, 2010

prepared by:
UR3.01, Resp. Roberto Basili, INGV, Sezione di Sismologia e Tettonofisica

UR3.01, Vanja Kastelic, Pierfrancesco Burrato, INGV, Sezione di Sismologia e Tettonofisica
URT.02, Chiara D'Ambrogi, ISPRA, Servizio Geologico d'Italia/Dipartimento Difesa del Suolo
UR 5.03, Michele M.C. Carafa, Salvatore Barba, INGV, Sezione di Sismologia e Tettonofisica

1. Description of the Deliverable

This deliverable contains three different products: one table with reclassified slip rate data from DISS, one table with slip rate values calculated from numerical models, and two study cases that illustrate the applications of original methods to estimate slip rate.

1) Geological slip rates.

Slip rates are commonly estimated in a variety of ways, depending on local tectonic setting, availability of data, investigators' skills, and other contingent factors. Slip rates are also very difficult to obtain, therefore any type of estimation is usually regarded as "great" value. In seismic hazard applications there is a need of having data collected in a homogeneous way. In addition, slip rate should imagine the behavior of faults at seismogenic depth and encompass a number of seismic cycles. The table below was designed to take into account all these circumstances in order to develop a standard in collecting slip rate estimations. The table is also designed to become a relational table for the DISS (Basili et al., 2008). These data are made available as a georeferenced file.

Data field	Definition
#CSS	*Ordinal of CSS*
#ISS	*Ordinal of ISS on an ISS row or number of associated ISS on a CSS row*
ID	*DISS-ID*
Name	*Source name*
Lon	*Source centroid or observation longitude*
Lat	*Source centroid or observation latitude*
StrikeMin	*As in DISS*
StrikeAvg	*Calculated*
StrikeMin	*As in DISS*
DipMin	*As in DISS*
DipAvg	*Calculated*
DipMax	*As in DISS*
RakeMin	*As in DISS*
RakeAvg	*Calculated*
RakeMax	*As in DISS*
SlipRate	*As in DISS*
Qualifier	*As in DISS*
North	*North-South component (positive northward)*
East	*East-West component (positive eastward)*
Vertical	*Vertical component (positive up)*
Lateral	*Strike-parallel component (positive right)*
Heave	*Normal-to-strike component (positive extensional)*
Dip-parallel	*Dip-parallel component (positive downdip)*
Rake-parallel	*Rake parallel component (absolute value)*
Surface/Depth_(S/D)	*S=Surface if observed/measured at ground surface; D=Depth if observed/measured at seismogenic depth*
Seismic/Total_(S/T)	*S=Seismic if it approximate a coseismic value; T=Total if approximate seismic+aseismic value*
Scale_of_observation	*Exponent of observational scale in meters. Integer. E.g. 3 means 1000 m; -3 means 0.001 m. NaN means Not a Number (null value).*
Method	*Short description of observation method. E.g paleoseismic trenching.*
Age_of_marker_name	*Geological age of marker used to make the estimate.*
Age_of_marker_min_y	*Minimum geological age of marker used to make the estimate in years, use scientific notation.*

Age_of_marker_max_y	*Maximum geological age of marker used to make the estimate in years, use scientific notation.*
Age_class_exponent	*Age class is defined as a power of ten. Integer value. E.g. 3 means 1000 y.*
Age_of_fault_name	*Geological age of fault activity inception.*
Age_of_fault_max_y	*Maximum geological age of fault activity inception in years, use scientific notation.*
Inversion	*Logical value. T=True; F=False. Indicate if fault was reactivated in a different tectonic regime.*

For fields defined as "As in DISS" see Basili et al. (2009).

In this table slip rate was broken down into its basic geometrical (Fig. 1.1), observational, and temporal components. We found the vertical component to be the most common. North and East components could be common for GPS measurements, but in this database version we found these components already converted into some other form. Taking into account the fault geometry, all components must be converted into rake-parallel slip for correct use. A recommendation for the future is to keep the original data unadulterated so that the rake-parallel value can be easily recalculated if the geometry of fault changes.

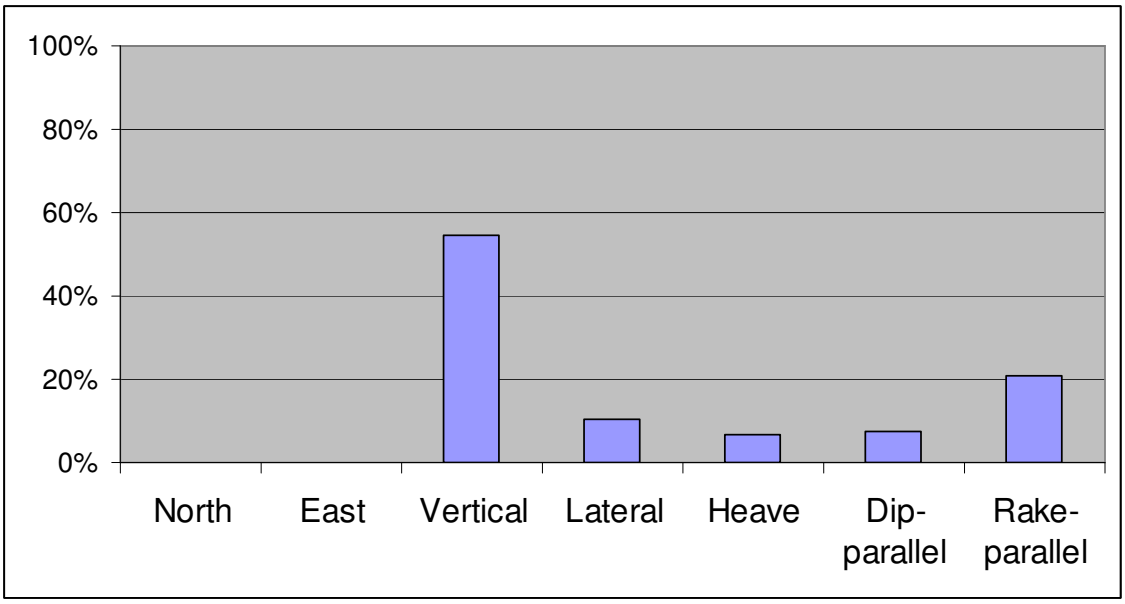

Fig. 1.1 – Histogram showing frequency (%) of different geometrical components used to estimate slip rate.

In 17% of all cases slip rate can be considered a proxy for seismic slip over time; the remaining 83% refers to total slip which includes interseismic and aseismic slip. This suggests that a strategy is needed to estimate seismic vs. aseismic ratio.
In 71% of all cases slip rate was determined from observations at the ground surface. Only the remaining 29% of cases refers to slip at seismogenic depth. This suggests developing a strategy to correct most slip rate values for the behavior at seismogenic depth.
Slip rate values so far collected are very much heterogeneous also in terms of the observational scale which varies from decimeters (such as that of trench logs) to hundred of kilometers (such as that of geodynamic models) and temporal scale which varies from few years (such as with GPS measurements) to few millions of years (long-term geological markers). We also noted whether the activity of faults refer to a reactivation of older faults with opposite movement type which may affect the frictional behavior.

2) Model-predicted slip rates and fault kinematics.
(Collaboration with UR 5.03 Megna)
The table is composed of 98 records, one for each CSS in the DISS 3.1.0. For 87 CSS the slip rate was successfully determined, 11 were not determined because of numerical instabilities or poor data coverage. Slip rate average is 0.39 mm/yr, while the mean of the standard deviation is 0.26 mm/yr. Figure X shows results in map view. These data are made available as a georeferenced file. The table structure is shown below.

Data field	Definition
IDSource	*Identifier code of the Composite Seismogenic Source (DISS v. 3.1.0)*
SourceName	*Composite Seismogenic Source name*
SLIPRATE(mm/yr)	*Average model-predicted slip rate in mm/y (NaN = -99999.00)*
STDEV(SLIPRATE)(mm/yr)	*standard deviation of model predicted slip rates in mm/yr*

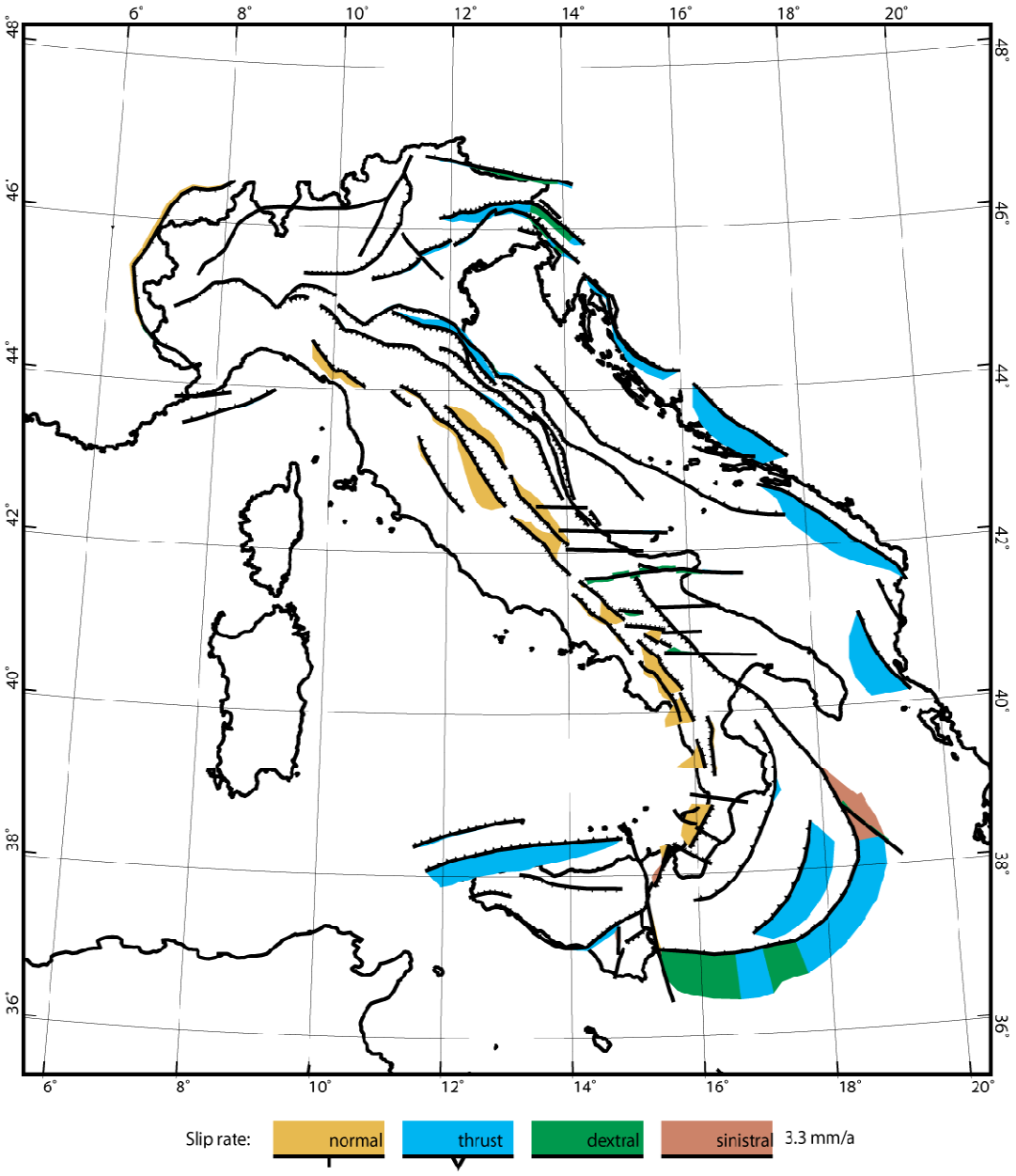

3) Original studies on slip rate determination.

3.1) Amatrice Basin (Central Apennines): normal faulting.

(Collaboration with UR T.02)

The Amatrice Basin occupies the northern part of a broad NNW-SSE stretching depression that includes, to the south, the Campotosto basin. The entire depression is bounded on the eastern side by the Mt. Gorzano normal fault that seems to have determined its formation and controlled its subsequent development. This fault is also considered to be presently active and potentially seismogenic (Blumetti et alii, 1993; Galadini & Galli, 2003; Boncio et alii, 2004).

The catchment area of the Amatrice basin is mostly developed on the Mt. Gorzano fault hanging wall (Fig. 2.1). The relative movement - eastern side up - on the West-dipping Mt. Gorzano fault determined the Marne con Cerrogna (calcareous marls and marls; Burdigalian-Tortonian) and Marne a Pteropodi (marls; Tortonian-Messinian) formations to become exposed on its foot wall. Except for a small sector on its far western edge, the rest of the catchment area is dominated by the Laga formation (Messinian), a quartz-rich sandstone dominated succession (Corda & Morelli, 1996). Significant continental deposits are only found on the eastern side of the catchment, in a small sector between the Tronto River (the main river of the basin) and the trace of the Mt. Gorzano fault. Because of the lack of elements for direct dating, their age is poorly constrained and based only on regional correlation with other Apennines intermontane basins. Generally, these continental deposits have been subdivided into three depositional units, one of which is proportionally very minor and scattered, that are attributed to the Lower Pleistocene - Upper Pleistocene (Cacciuni et alii, 1995).

To gain insight into the long-term activity of the Mt. Gorzano fault and its role in controlling the evolution of the Amatrice basin, we carried out a stratigraphic and geomorphic analysis of the continental deposits.

We positively identified two clastic continental units within the main depositional body that filled up the Amatrice basin. Just downstream from the River Tronto head, the steep valley walls of a deeply incised gorge provide a comprehensive exposure of the lower and older unit. This is a coarse, moderately rounded, gravel-to-cobble, clast-supported, up to 30 meters thick conglomerate. Its composition is almost exclusively made up of arenaceous clasts derived from the Laga formation. Occasionally, the sedimentary fabric suggests a roughly south-to-north direction of transport.

The higher and younger unit is exposed near the top of the Tronto River gorge and in a number of stream incisions and road cuts. This is a coarse, moderately rounded, gravel-to-cobble, clast-supported, up to 10 meters thick conglomerate with interspersed boulders. Its composition is predominantly made up of arenaceous clasts derived from the Laga formation but the calcareous component derived from the Marne con Cerrogna formation is clearly identifiable and measurable (Fig 2.2). The chaotic fabric and the reduced level of clast roundness suggest a very local sediment supply from the near slope to the East of the basin. This deposit evolves gradually upward into coarse-to-fine, variously weathered, eluvial sand and to the top soil. Its top depositional surface coincides with a broad plateau, occasionally overlain by younger debris fans.

Our preliminary estimations show that the relative content of the calcareous component within the younger unit is of about 5-6%. This is a lower limit because we ignore the relative content within the matrix that we assigned by default to the arenaceous component. A more detailed provenance analysis of the calcareous component shows that a significant number of clasts were derived from the lower and older portion of the Marne con Cerrogna formation. The relative content between arenaceous and calcareous components in the source area, i.e. the mountain slope on the eastern side of the basin, is about 7-16%.

Considering all sources of uncertainty in these estimates, including that the calcareous clasts are more subject to chemical weathering than the arenaceous clasts, we can consider the relative abundance of calcareous rock in the source area and within the continental deposit to be rather similar to one another. This implies that the Marne con Cerrogna formation should have been already exposed at the time when the continental unit at the top of the Amatrice basin infill was deposited. We suggest that the careful estimation of these relative abundances will help provide an estimate of the relative increment of geological displacement on the Mt. Gorzano fault and the resulting increment in the Marne con Cerrogna formation exposure since the time of depositional abandonment of the younger continental unit.

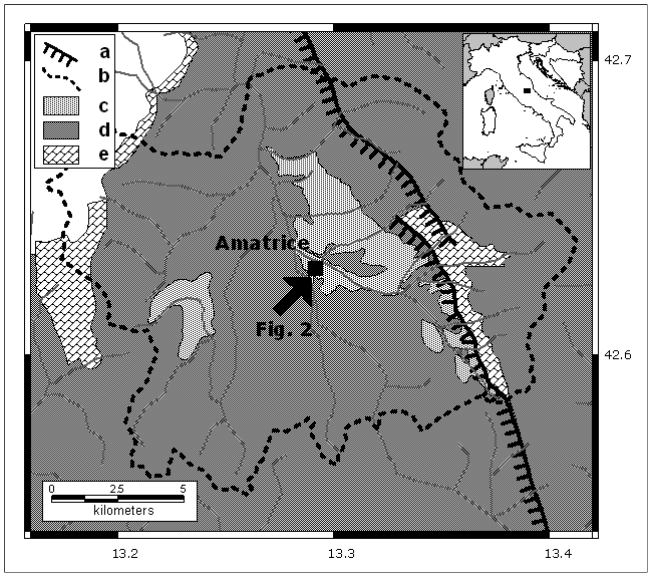

Fig. 2.1 – Geological sketch map of the Amatrice basin. Legend: a) normal fault; b) catchment limit; c) Continental deposits (Quaternary); d) Laga formation (Messinian); Marne a Pteropodi (Tortonian-Messinian) and Marne con Cerrogna (Burdigalian-Tortonian) formations. Arrow points at the location of the Quaternary deposit exposure shown in figure 2.

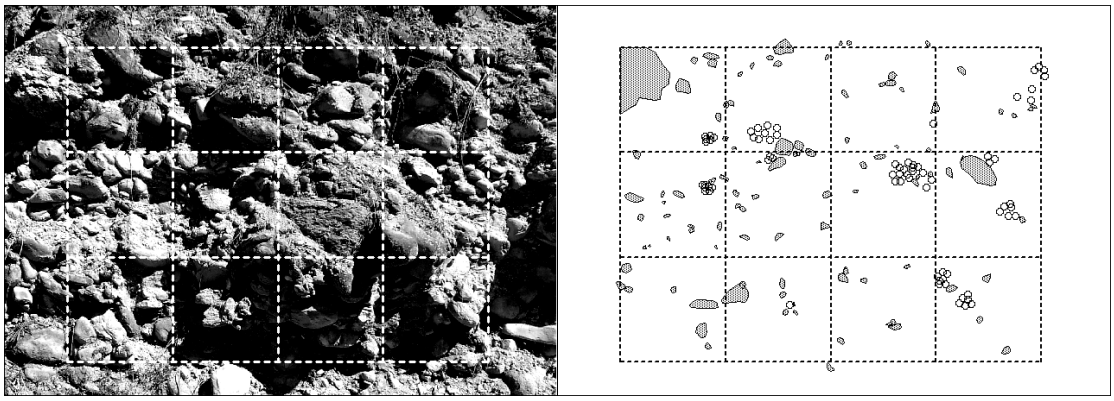

Fig. 2.2 – Left: exposure of the Quaternary continental deposit of the Amatrice basin infill (See figure 1 for location). Right: clasts of the Marne con Cerrogna formation are outlined; circles indicate clasts of about 1 cm in diameter. Each square of the grid in the foreground of both panels is 50x50 cm.

3.2) Emilian Arc (Northern Apennines): reverse faulting.
(Collaboration with UR T.02 and UR 3.11 in the framework of the "Training course of the Geological Survey of Italy - ISPRA", Session 2009, Rome.)

This section illustrates an example about how to correct slip rate estimations in a contractional tectonic environment where the thrust fault is buried below a thick sediment cover.
In order to calculate the long-term (Pliocene-to-Holocene) geological slip rate of the thrust underlying the buried fold of the Emilian Arc, we made a 3D reconstruction of its central portion along a NNE, 50-km long swath profile, running from the outcropping thrust wedge to the south and including the outermost buried anticlines of the Northern Apennines to the north (Fig. 3.1). This approach is similar to that used by Scrocca *et alii* (2007). The data used here were taken from the activity of RU 3.11 and from publicly available subsurface datasets.

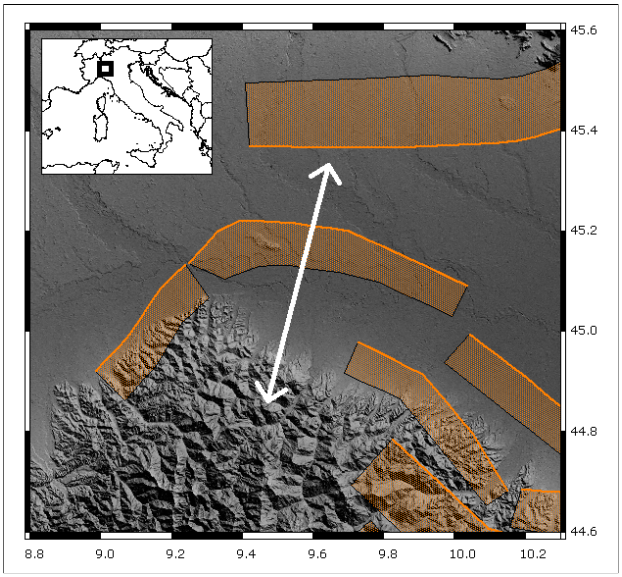

Fig. 3.1 – Map location of the profile across the Emilia Arc in figure 4 with the DISS 3.1.0 composite seismogenic sources for reference.

The 3D subsurface geometry of pre- and syn-tectonic strata (Fig. 3.2) was built by using for the deep portion of the model the structural surfaces derived from geological cross-sections by Toscani *et alii* (2006) constrained by the stratigraphy of deep oil well logs. The shallow portion of the model was derived by the stratigraphic data used for the reconstruction of the regional aquifers by RER & ENI-Agip (1998) and Regione Lombardia & Eni (2002).
A decompaction workflow was applied to the reconstructed 3D model in order to remove the effects of rock volume change due to porosity reduction with time. Vertical decompaction is obtained by progressively backstripping the depositional horizons and thereby allowing the underlying rocks to expand as a result of the overburden removal.
Using algorithms supplied by the software package Move (MVE, Ltd) we restored the effects of the compaction history for the aquifer horizons dated at 0.45 My, 0.65 My, 0.8 My and for the top of Pliocene (1.8 My) and Messinian (5.3 My). The decompaction was performed with the 3DMove *Decompaction tool*, using the flexural isostasy setting and assuming a sub-aerial load for the two uppermost aquifers (A: 0.45 My and B: 0.65 My) and a submarine load for the deepest aquifer (C: 0.8 My) and the underlying Pleistocene (1.8 My) and Pliocene deposits (5.3 My).
We made the slip rate calculations for the unfaulted horizons using two methods that gave comparable results (Table 3.1): 1) an elastic half-space dislocation modeling of surface

deformation, and 2) a trishear fault propagation modeling (*Trishear algorithm* in 2DMove). To better describe the evolution of main thrust we calculated the slip rate also on the faulted horizons (top Pliocene and top Messinian); the calculation was extended to the whole 3D model to verify the lateral variations along the thrust. The *Separation tool* in 3DMove was used to measure the heave, throw and slip between fault cutoffs.

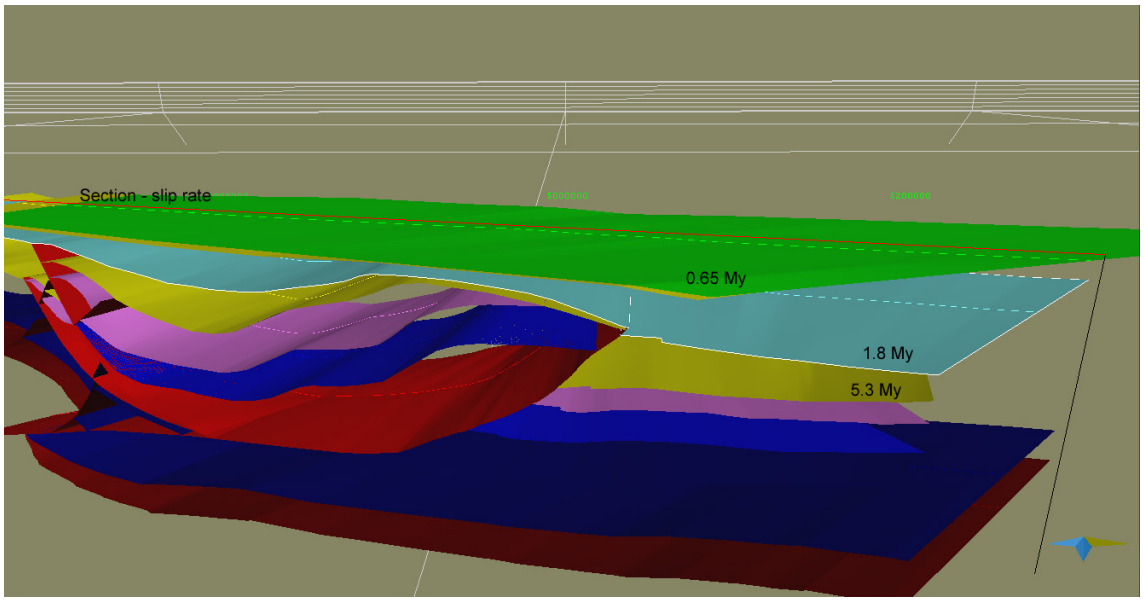

Fig. 3.2. – 3D-geological model of the central portion of the Emilian Arc (the main thrust in the figure). The red line is the swath NNE oriented used for the slip rate calculations for the unfaulted horizons (the upper aquifer is not visible in the figure), the yellow surface beneath the green is dated at 0.8 My.

Table 3.1: Slip rates were calculated using age of horizons and either the net displacement or the vertical topographic contrast (vertical separation) between the crest of the anticline and the hinge of the syncline. In the second case we used elastic half-space dislocation modeling of surface deformation to derive the slip on the thrust fault plane. All the calculations were performed after decompaction correction of the geometry of the horizons.

Horizon	Age (My)	Dip-parallel Throw (m)	Vertical Separation (m)	Progr. Slip (m)	Progr. Slip Rate (mm/y)	Interval Slip Rate (mm/y)
A	0.45	-	10	22	0.05	0.05
B	0.65	-	27	58	0.09	0.18
C	0.80	-	39	84	0.11	0.17
base Pleistocene	1.8	167	-	167	0.09	0.08
base Pliocene	5.3	3751	-	3751	0.7	1.02

2. Relevance for DPC and/or for the scientific community

Slip rate is a fundamental parameter in fault characterization which has a dramatic influence on probabilistic seismic hazard calculations. Slip rate is also very difficult to estimate. As of today, little attention has been given to differentiating slip rates in terms of the method used to estimate it, of the involved time window, and of the implicitly assumed behavior of the fault.

This information will play a role when attempting to compare deformation rates based on instrumental data or models with geologic slip rates.
The slip rate table presented here is one of the first efforts made at developing a standardized method to collect geological slip rates and store them in a database. The structure of this table complies with prescriptions given in Basili et al. (2009), as such it can be easily incorporated as a relational table in the DISS. The usage of this standardized method will ensure that slip rate values are used in a homogeneous way in PSHA that use slip rate as input. This standardized method could be shared with other similar efforts at European (SHARE) and worldwide (GEM) scale.
In addition, the long-term (anelastic) slip rate completes the seismogenic fault map, the dataset of geodetic velocities and the catalogue of historical seismicity, and is to be used, together with the map of anelastic strain rate, as the basis of regional seismic hazard studies.

3. Changes with respect to the original plans and reasons for it

There are no significant changes to the original plans.

4. References

Basili R., G. Valensise, P. Vannoli, P. Burrato, U. Fracassi, S. Mariano, M.M. Tiberti, E. Boschi, The Database of Individual Seismogenic Sources (DISS), version 3: summarizing 20 years of research on Italy's earthquake geology. Tectonophysics, 2008. 453, 20-43, doi:10.1016/j.tecto.2007.04.014.

Basili, R., Kastelic, V., Valensise, G., and DISS Working Group 2009, 2009, DISS3 tutorial series: Guidelines for compiling records of the Database of Individual Seismogenic Sources, version 3. Rapporti Tecnici INGV, no. 108, 20 p., http://portale.ingv.it/produzione-scientifica/rapporti-tecnici-ingv/archivio/rapporti-tecnici-2009/

Blumetti A.M., Dramis F., & Michetti A.M. (1993) – Fault-generated mountain fronts in the central Apennines (central Italy): geomorphological features and seismotectonic implications. Earth Surface Processes and Landforms, 18, 203-223.

Boncio P., Lavecchia G., Milana G. & Rozzi B. (2004) – Seismogenesis in Central Apennines, Italy: an integrated analysis of minor earthquake sequences and structural data in the Amatrice-Campotosto area. Annals of Geophysics, 47, 1723-1742.

Cacciuni A., Centamore E., Di Stefano R. & Dramis F. (1995) – Evoluzione morfotettonica della Conca di Amatrice. Studi Geol. Camerti, Vol. Spec. 2, 95-100.

Corda L. & Morelli C. (1996) – Compositional evolution of the Laga and Cellino sandstones (Messinian-Lower Pliocene, Adriatic foredeep). Boll. Soc. Geol. It., 115, 423-437.

Galadini F. & Galli P. (2003) – Paleoseismology of silent faults in the Central Apennines (Italy): the Mt. Vettore and Laga Mts. faults. Annals of Geophysics, 46, 815-836.

Regione Emilia-Romagna & Eni-Agip (1998) – Riserve idriche sotterranee nella Regione Emilia-Romagna. A cura di G. Di Dio. S.EL.C.A., Firenze.

Regione Lombardia & Eni (2002) – Geologia degli Acquiferi Padani della Regione Lombardia. A cura di C. Carcano & A. Piccin .S.EL.C.A., Firenze.

Scrocca D., Carminati E., Doglioni C. & Marcantoni D. (2007) – Slab retreat and active shortening along the central-northern Apennines. In: Lacombe O., Lavé J., Roure F. & Verges J. (Eds.), Thrust belts and Foreland Basins: from fold kinematics to hydrocarbon systems. Frontiers in Earth Sciences. Springer, 471–487.

Toscani G., Seno S., Fantoni R. & Rogledi S. (2006) - Geometry and timing of deformation inside a structural arc: the case of the western Emilian folds (Northern Apennine front, Italy). Boll. Soc. Geol. It., 125 (2006), 59-65.

5. Key publications/presentation

Barba, S., M.M.C. Carafa, and E. Boschi E. (2008), Experimental evidence for mantle drag in the Mediterranean, Geophys. Res. Lett., 35, L06302, doi:10.1029/2008GL033281.

Barba, S., R. Basili, M. M. C. Carafa, and F. Balestra (2008), Depth of the seismogenic layer in Italy, American Geophysical Union, Fall Meeting 2008, abstract #T51D-04.

Basili R. and D'Ambrogi C. (2010). Provenance of the Amatrice Basin (central Apennines) infill: implications for the long-term activity of the Mt. Gorzano fault. Abstract for the 85th Congresso della Società Geologica Italiana, L'appennino nella Geologia del Mediterraneo Centrale, 6-8 September, 2010, Pisa.

Carafa M. M. C., S. Barba (2009), S1 - RU 5.03:Strenght of the lithosphere and strain rate in the Northern Apennines, 1st annual meeting of Seismological Projects, 19-21 October 2009, Rome, http://portale.ingv.it/l-ingv/progetti/progetti-finanziati-dal-dipartimento-di-protezione-civile-1/progetti-dpc-convenzione-2007-2009/progetti-s/first-annual-meeting/.

Maesano F., D'Ambrogi C., Burrato P. and Toscani G. (2010). Long-term geological slip rates of the Emilia thrust front (Northern Apennines) from 3D modeling of key buried horizons. Abstract for the 85th Congresso della Società Geologica Italiana, L'appennino nella Geologia del Mediterraneo Centrale, 6-8 September, 2010, Pisa.